Progress report on the catalyst layers for hydrocarbon-fueled SOFCs

Panpan Zhang[a], Zhibin Yang[a, *], Yiqian Jin[a], Changlei Liu[b], Ze Lei[a], Fanglin Chen[c, *], Suping Peng[a]

[a] *Research Center of Solid Oxide Fuel Cell, China University of Mining & Technology-Beijing, Beijing 100083, China*

[b] *CHN ENERGY Renewable Co., Ltd, Beijing 100000, China*

[c] *Department of Mechanical Engineering, University of South Carolina, Columbia, SC 29208, USA*

[*] E-mail address: yangzhibin0001@163.com (Z. Yang); chenfa@cec.sc.edu (F. Chen)

Abstract

Solid oxide fuel cell (SOFC) is an energy conversion device that can directly convert the chemical energy of carbonaceous fuels into electricity. Solving the problem of carbon deposition in the conventional nickel-based anode is essential to improving the performance of SOFC when operating on carbonaceous fuels. Although impressive progress has been made in the development of alternative anode materials, nickel-based anodes with superior catalytic activity for carbonaceous fuels are still the most promising anode for the commercialization of SOFCs. The deposition of a catalyst layer with high catalytic activity for carbonaceous fuels over the nickel-based anode has been demonstrated as an effective way to enhance the performance and long-term stability of hydrocarbon-based SOFC. This review introduces the working principles of the catalyst layers, discusses the recent progress of the catalyst layer materials for hydrocarbon-fueled SOFC and issues of the different catalyst layer materials. Finally, some of the future prospects and challenges of the catalyst layers are summarized in this review article.

Key words: solid oxide fuel cell; nickel-based anode; carbonaceous fuel; **catalyst layer**

1. Introduction

As an efficient energy conversion device, fuel cells have shown the capability in the clean utilization of energy[1]. In particular, solid oxide fuel cells (SOFCs) are fuel flexible [2], and can utilize various fuels including hydrogen, methane, propane, alcohol[3], ammonia[4, 5], carbon monoxide [6] and even solid carbon[7, 8]. This fuel flexibility broadens the applications of SOFCs from hydrogen to hydrocarbon-based fuel [9]. Due to the excellent electronic conductivity, good compatibility with the common electrolyte materials, and high catalytic activity for hydrogen and hydrocarbon-based fuel, nickel-based cermet has been widely applied as SOFC anode materials [10-12]. However, the superior catalytic activity for C-H bond dissociation and C-C bond formation on the nickel-based anode can quickly lead to carbon deposition when operating in hydrocarbon-based fuel. Carbon deposition can severely damage the catalytic activity of Ni, reduce the density of the three-phase boundary (TPB), and deteriorate the performance of SOFCs (Fig.1) [13, 14].

In order to alleviate the carbon deposition issues, different approaches have been explored to mitigate the coking problems on nickel-based anodes. The most straightforward method to suppress coke formation is via a thermodynamic approach that involves the addition of oxygen-containing gas into the fuel to increase the O/C ratio [15] at the cost of sintering of nickel particles and decrease in anode catalytic activity [16]. Other strategies to moderate or to remove carbon deposition over the nickel-based anodes include alloying nickel with a second metal [17], using oxides for Ni surface modification [18], adopting nickel-free cermet anodes [19], and using

perovskite-type oxides as anode materials [20]. However, the above methods also present issues that have restricted the further application of SOFCs. For example, the low conductivity of perovskite-type oxides in the reducing atmosphere causes serious current collection problems in SOFC applications. The low catalytic activity for hydrocarbon fuel of perovskite-type oxides can reduce the power outputs of SOFCs [21, 22]. As for the Cu-based anodes, the fabrication of anodes is more complicated and costly due to the melting point difference between Cu (1083 ℃) and Ni (1453 ℃) [23, 24].

Different from the methods mentioned above, applying a catalyst layer to mitigate the carbon deposition on nickel-based anode while maintaining its advantages is an appealing option to achieve a stable operation of SOFCs in hydrocarbon-based fuel [25]. The deposition of a catalyst layer with high catalytic activity for hydrocarbon-based fuel over the nickel-based anode has been proved to be an effective way to suppress carbon deposition on the anode. This method was proposed by Zhan and Barnett who introduced Ru/CeO_2 as a catalyst layer to increase the stability of SOFCs by converting iso-octane/CO_2/steam/air mixture into syngas [26], paving the way for many other materials that have been investigated as the catalyst layer. In this review, the recent development of the catalyst layer material in the traditional Ni-based SOFC anode is provided, and the future prospects and challenges of the catalyst layers are summarized, which would contribute to the development of hydrocarbon-based SOFCs.

2. Working principles of the catalyst layers

There are mainly two structural forms of the SOFC anode catalyst layers. One is directly deposited on the surface of the SOFC anode (Fig. 2), and the other is located close to but separated from the anode, independent from the entire cell (Fig. 3). The carbonaceous fuels first pass through the catalyst layer and then diffuse to the anode. As for CH_4/H_2O fuel, CH_4 and H_2O are firstly converted by the catalyst layer into CO and H_2 following steam reforming of CH_4 (Eq (1)), and then diffuse into the anode in which the electrochemical oxidation reaction takes place. The electrochemical reaction products (H_2O and CO_2) continue to react with CH_4 according to Eq (1) & (2) when passing through the catalyst layer, generating CO and H_2. Based on theoretical and experimental studies, direct electrochemical oxidation of CH_4 is more difficult than that of CO and H_2 [25, 27]. Therefore, the cells′ performance with a catalyst layer is higher than that of the conventional one.

$$CH_4 + H_2O \rightarrow CO + 3H_2 \quad (1)$$

$$CH_4 + CO_2 \rightarrow 2CO + 2H_2 \quad (2)$$

The anode catalyst layer can reduce the diffusion rate of the fuel into and electrochemical reaction products out of the anode, hence effectively increasing the concentration of the electrochemical reaction products in the anode with higher O/C ratio, and the rate of the formation of carbon deposits is mitigated [28].

3. The classification of the catalyst layers

3.1. The direct-loaded catalyst layers

3.1.1. Noble metal-based materials

There have been many studies on the noble metal-based catalysts such as Ru, Ag, Ir, and Pd for SOFC applications [29-32]. Barnett et al. [26] pioneered the study of the effect of the catalyst layer on the performance of SOFCs. A Ru/CeO_2 catalyst layer was directly deposited on the surface of Ni-YSZ anode. This catalyst layer could effectively catalyze the reforming of iso-octane without coke formation, which prevented the Ni-YSZ anode from being directly exposed to iso-octane. The cell with a Ru/CeO_2 catalyst layer yielded a peak power density (PPD) of ~600 mW/cm^2 at 770 °C when operated on iso-octane/air/CO_2 fuel and successfully operated at a constant current load of 0.6 A/cm^2 for ~50 h with 6% iso-octane/94% CO_2 fuel. In comparison, the cell without the Ru/CeO_2 catalyst layer was deactivated quickly and failed after 10 h of operation when operated at a constant current load of 0.9 A/cm^2. This work demonstrated a novel method to mitigate the problem of carbon deposition in the nickel-based anode and significantly promoted the development of carbon-based SOFCs [33-36]. However, as pointed by the authors, one disadvantage in the catalyst layers was that it reduced the rate at which fuel could diffuse to the anode, therefore decreasing the cell′s power output.

To tackle this problem, flower-like mesoporous CeO_2 microsphere (1-3 μm) (Fig. 4) was investigated for SOFCs [37]. Ru was loaded on it by an impregnation-reduction method. Compared with Ru/CeO_2 prepared by Barnett et al.[26], the distribution of Ru

on flower-like mesoporous CeO_2 was more uniform, which could effectively suppress the sintering and agglomeration of Ru particles. Moreover, this CeO_2 microstructure could facilitate gas diffusion and extend the TPB length. Operated with 5% iso-octane/9% air/3% H_2O/83% CO_2 fuel, the cell with this catalyst layer yielded a PPD up to 654 mW/cm^2 at 600 °C. Compared with the results reported by Barnett et al., the cell′s performance with this catalyst layer was noticeably improved under the same operational conditions. The results demonstrated that the concentration polarization could be avoided by optimizing the catalyst layer.

Ceria oxide has been found to be an excellent highly active catalyst for hydrocarbon oxidation and cracking and the above results demonstrated that the catalytic activity for hydrocarbon oxidation could be greatly improved through the mesoporous ceria as compared to the bulk ceria. Therefore, Wang et al. [38] synthesized mesoporous $Ce_{0.8}Sm_{0.2}O_{1.9}$ (SDC) oxide by a novel glycine-nitrate combustion process with in situ created nickel oxide as a template. This SDC powder with 7 wt% Ru was subsequently deposited onto the anode surface as the catalyst layer. The highly porous structure of the Ru/SDC catalyst layer enabled facile gas diffusion inside the Ru/SDC catalyst layer. Consequently, the concentration polarization was not observed. The cells with and without the catalyst layer showed comparable performances at intermediate temperatures when operated on H_2 fuel, suggesting that this catalyst layer had no impact on the performance of the cell when operated on H_2. Additionally, the cell with a Ru/SDC catalyst layer displayed favorable performance with a PPD of ~462 mW/cm^2 at 650 °C operating on wet CH_4 (3 mol% H_2O) fuel. The value of the PPD was 25%

higher than that of the conventional cell without the Ru/SDC catalyst layer. Nobrega et al. [39] loaded 0.1 wt% Ir on $Ce_{0.9}Gd_{0.1}O_{2-x}$ (CGO) through the impregnation method and used it as the catalyst layer material for direct-ethanol SOFCs. The Ir/CGO catalyst exhibited high catalytic activity for hydrocarbon reforming reactions. By optimizing the operational conditions, the cell with an Ir/CGO catalyst layer could operate for 650 h with excellent stability at 850 °C using ethanol/nitrogen (10/90%) as the fuel. Considering a significant part of ethanol has been pyrolyzed before reaching the catalyst layers at the SOFC operating temperature, the primary pyrolysis products were still effectively converted by the catalyst layer. Thus, the degradation of the cell due to carbon deposition was avoided. Although the cell exhibited excellent operational stability in the ethanol fuel, the authors did not investigate and compare the cell′s electrochemical performance with or without the deposition of the catalyst layers.

Pd has been demonstrated as the most efficient electrocatalyst for hydrocarbon oxidation. Compared with Pt, Pd is more abundant and lower-cost. Nano-sized Pd catalysts can enhance the electrochemical activity of Ni-based anodes toward the oxidation of hydrogen and hydrocarbon fuels and suppress carbon formation. A nano-scale flower-like Pd catalyst layer (10 μm) was prepared on the Ni-YSZ anode surface by galvanic displacement reaction using acetone as a surfactant [40]. The catalyst layer with Pd nanoparticles could increase the effective TPB of electrochemical reaction and enhance the electrical conductivity of the anode. The cell with this catalyst layer yielded a PPD of 196 mW/cm^2 at 750 °C operating on ethanol. The value of the PPD was 28% higher than that of the conventional cell. Furthermore, for the cell with a catalyst layer,

reasonable stability was maintained for 59 h under OCV condition, while it sharply failed after 6 h of operation for the conventional one when operated on ethanol. This was because the catalyst layer with Pd nanoparticles could act as a diffusion barrier layer and effectively depress the carbon deposition on the surface of Ni-based anode. Their findings showed that the catalyst layer could be an effective way to enhance the operational stability and performance of hydrocarbon-based SOFCs.

Although noble metal-based catalysts are desirable as the catalyst layer materials because of their excellent catalytic activity and good coking resistance, the high price has made an obstacle towards its large-scale commercial application. Therefore, development of cheap and highly active materials for the catalyst layer is critical. Furthermore, the stability of the noble metal-based catalysts during the long-term operation is also a pressing issue to be solved [10, 41, 42]. One of the significant strategies is to use the in-situ exsolution method [32, 43-47]. In this way, noble metal-based catalysts can be incorporated into the B site of the perovskites, and then partly exsolved as nanoparticles on the surface of the substrate in reducing atmosphere. The size distribution and morphology of the exsolved nanoparticles are more uniform, and agglomeration of the catalysts can be effectively mitigated [43, 44].

3.1.2. Nickel-based materials

The prospects of noble metal-based catalysts in commercial SOFC applications are not feasible due to the high cost and instability under long-term operation. Nickel-based catalysts have been extensively used due to their low cost, high catalytic activity

and abundant reserves. Wang et al. [48] developed a γ-Al_2O_3 supported nickel catalyst layer (Ni/Al_2O_3) in CH_4-fueled SOFCs. According to the catalytic tests, the Ni/Al_2O_3 exhibited equivalent catalytic activity to Ru/CeO_2 and better catalytic activity than the anode material (Ni/ScSZ) for partial oxidation, steam and CO_2 reforming of CH_4 within all test temperature ranges. Also, Ni/Al_2O_3 exhibited better thermal-mechanical compatibility than that of Ru/CeO_2. For the cell with the Ni/Al_2O_3 catalyst layer, the gas diffusion limitation in the catalyst layer decreased the CH_4 content while increased the product content in the anode. Moreover, the effluent gases (CO_2 and H_2O) from the anode could also reform CH_4 on the catalyst layer into syngas, which could further improve the electrochemical performance of the cells. The PPD of the cell with this catalyst layer reached 382 mW/cm^2 at 850 °C when operated on pure CH_4 fuel. The operational reliability demonstrated that the cell with a catalyst layer was more stable than the conventional one. The PPD of the cell with this catalyst layer reduced about 3% of the initial value when operated on CH_4 for 90 min, while the decrease in the PPD was about 41% in the conventional one under similar testing conditions. Consequently, the application of the Ni/Al_2O_3 on the anode surface significantly improved the performance of the cell.

However, O_2-TPO analysis indicated that Ni/Al_2O_3 was still prone to suffering from carbon formation during the long-term operation. It is necessary to further improve the coking resistance of the nickel-based catalysts. It has been shown that the catalytic activity and coking resistance of nickel-based catalysts are strongly related to supports and promoters [49, 50], and it seems that some lanthanum ions or alkaline

metal ions are excellent promoters for nickel-based catalysts, which can effectively improve the interaction between the catalysts and the supports. In addition, they can also improve the dispersion and surface physicochemical properties of the catalysts. Wang et al. [51] investigated the effects of Li_2O, La_2O_3, and CaO promoters on the catalytic activity and coking resistance of Ni/Al_2O_3 and found that the introduction of promoters effectively improved the basicity of the catalyst surface, and enhanced the interaction between NiO and Al_2O_3 as well as the dispersion of NiO. Among the various catalysts, $LiLaNi/Al_2O_3$ displayed the highest catalytic activity and stability. The amount of carbon deposited over $LiLaNi/Al_2O_3$ was only 18.5% as compared to that of Ni/Al_2O_3 in pure CH_4 fuel for 5 min at 850 °C. Although the coking resistance of Ni/Al_2O_3 was significantly improved in the short term, the evaporation of surface lithium under long-term operation was a newly emerging challenge, which would decrease the surface basicity and further trigger the problem of carbon deposition in SOFCs. Therefore, $Li_{0.33}La_{0.56}TiO_3$ (LLTO) was developed as the support for the Ni-based catalysts. Compared with the $LiLaNi/Al_2O_3$ catalyst, Ni/LLTO exhibited much higher Li^+ conductivity, and the lithium evaporation on the surface of LLTO could be compensated by the lithium diffused from the bulk. Consequently, the Ni/LLTO catalyst's surface basicity was more stable than that of $LiLaNi/Al_2O_3$ during long-term calcination at high temperature. The cell with a Ni/LLTO catalyst layer was quite stable for 160 h under a constant current load of 200 mA/cm^2 at 650 °C, while the cell with a $LiLaNi/Al_2O_3$ catalyst layer quickly failed after 55 h of operation. The result indicated that using a Li^+-conducting material as the support for a Ni-based catalyst layer could

be a novel approach to enhance coking resistance in direct-CH_4 SOFCs based on lithium compensation [52].

Although the problem of carbon deposition in the Ni-based catalyst layer has been temporarily alleviated, all the catalysts mentioned above displayed poor electrical conductivity. The electronic conductivity of the catalyst layer and the current collection of the cell must be considered in practical applications. Wang et al. [53] introduced Cu to LiLaNi/Al_2O_3 through physical mixing to improve the conductivity of the catalyst layer and this work was fairly promising. They discovered that when the mass ratio of LiLaNi/Al_2O_3 to Cu was 50:50, the surface conductivity of LiLaNi/Al_2O_3 (1.60 S/cm) was comparable to that of Ni-YSZ anode. Furthermore, the catalyst layer with the addition of Cu exhibited satisfactory coking resistance in CH_4 fuel, which was comparable to that of LiLaNi/Al_2O_3. When CH_4/O_2, CH_4/H_2O, and CH_4/CO_2 were applied as fuels, the cells with the catalyst layer yielded PPDs of 1081, 1036, and 988 mW/cm^2 at 850 °C, respectively, similar to the cells with a LiLaNi/Al_2O_3 catalyst layer in the same fuels. The result indicated that the conductivity of the catalyst layer could be effectively improved by introducing the right amount of Cu.

Recently, proton conductors such as $BaZr_{0.1}Ce_{0.7}Y_{0.1}Yb_{0.1}O_{3-\delta}$ (BZCYYb) have been reported to exhibit exceptional water storage capacity due to their high Fermi basicity and low electronic work function, and the absorbed water can facilitate CH_4 steam reforming and promote the oxidation elimination process of carbon deposition[22]. To further improve the catalytic activity and coking resistance of nickel-based catalysts, Zhao et al. [54] developed two kinds of catalyst layers,

$Ni/La_{1.95}Sm_{0.05}Ce_2O_7$ (LSDC) and $Ni/La_2Ce_2O_7$ (LDC). Both catalyst layers exhibited excellent water storage capability, which can significantly improve the performance of the SOFCs in CH_4 fuel. Compared with the traditional proton conductor material BZCYYb, LDC and LSDC displayed better stability in CO_2-containing atmospheres, thus ensuring the excellent stability of the catalyst layer materials during the long-term operation. In wet CH_4 at 650 °C, the PPD of the cell with the addition of Ni/LDC and Ni/LSDC was 699 ± 20 and 639 ± 20 mW/cm^2, respectively, while the PPD of the conventional cell was only 580 ± 20 mW/cm^2. As shown in Fig. 5, the cell with a catalyst layer was reasonably stable for 26 h under at a constant current load of 200 mA/cm^2 at 650 °C operating on wet CH_4, while the performance of the conventional cell dramatically failed after 10 h of operation under the same conditions.

Although the catalytic activity of nickel-based materials is comparable to that of noble metal-based materials, nickel-based catalysts are more likely to suffer from severe carbon deposition than noble metal-based catalysts [48]. Meanwhile, nickel particles are prone to sintering when operated at high temperatures for a long time, resulting in poor performance of this catalyst [12, 55, 56]. It is necessary to improve the sintering resistance of the nickel-based catalysts to ensure high catalytic activity to satisfy coking resistance. As mentioned above, the catalytic activity, sintering resistance, and coking resistance of nickel-based catalysts are strongly related to supports and promoters [57, 58]. The porous supports with large specific surface areas can improve the dispersion and sintering resistance of the nickel-based catalysts [25]. Moreover, the promoters can influence the interaction between the catalysts and the supports by

changing the acidity or basicity of the surface of the catalysts, thereby influencing the catalytic activity, sintering resistance, and coking resistance of the catalysts. Thus, the composition of nickel-based catalysts needs to be further optimized in the future to maintain the long-term operational stability of the cell using hydrocarbon fuels.

3.1.3. Copper-based materials

Copper has been known to neither dissolve carbon nor show catalytic activity for the promotion of C-C bond formation and C-H activation. Meanwhile, copper-based materials exhibit excellent chemical stability and high electronic conductivity, which can effectively solve the problem of current collection in SOFCs. CeO_2, with good catalytic activity for reforming reactions [59], was often added to improve the performance of copper-based catalysts due to their unsatisfactory catalytic activity in hydrocarbon-based fuel. Ye et al. [60] prepared a Cu/CeO_2 catalyst layer and directly deposited it to the anode surface by a screen printing method. As for the prepared catalyst layer, copper acted as current collector while ceria provided a high catalytic activity for hydrocarbon reforming. The addition of the Cu/CeO_2 catalyst layer to the supported anode surface could enhance the cell′s performance and coking resistance in ethanol fuel by pre-reforming ethanol. To ensure a strong binding between the catalyst layer and the anode, they studied the effect of different heat-treatment temperature on the cell performance. The cells with a Cu/CeO_2 (weight ratio 1:2) catalyst layer calcined at 1100 °C displayed both high power outputs and reasonable durability for 80 h without carbon formation when operated in ethanol-steam. It is well known that metal-

supported ceria is an effective catalyst for ethanol steam reforming. To further improving the activity of the Cu/CeO_2 catalyst for ethanol steam reforming, Al_2O_3 and ZrO_2 were incorporated in the Cu/CeO_2 catalyst to act as a promoter for ethanol steam reforming. The ethanol steam reforming (ESR) was enhanced due to high OH group surface mobility in Al_2O_3 and ZrO_2. In ethanol steam at 800 °C, the PPD of the cell with a Cu/CeO_2 catalyst layer was only 442 mW/cm^2, and increased to 493 and 519 mW/cm^2 with the addition of $Cu/(CeO_2\text{-}Al_2O_3)$ and $Cu/(CeO_2\text{-}ZrO_2)$ catalyst layers, respectively. However, the long-term stability of the cell was relatively unsatisfactory, as the cracking and the obvious delamination of the catalyst layer led to the decayed cell performance. To address this problem, Ni/CeO_2 was added as a transition layer between the Cu/CeO_2 catalyst layer and the anode. This transition layer could effectively match the thermal expansion coefficients of the other materials. The cells with this catalyst structure operated stably for 250 h in various fuels and temperatures (Fig. 6) [61]. Furthermore, the cells with the above catalyst layer structure also displayed a good performance when operating in H_2-CO syngas fuels. The cell showed excellent stability during 460 h operation in 48.5% H_2/48.5% CO/3% H_2O mixtures at 750 °C. However, carbon deposition still took place on the anode functional layer, and the cell performance decayed after 630 h of operation [62].

In addition, the copper-based catalyst layer can also be used for the single-chamber SOFC design that operates on a homogeneous mixture of fuel and oxidant gas. For example, $Cu/(ZnO\text{-}Al_2O_3)$ was investigated as catalyst layer for anode-supported single-chamber SOFCs operating on ethanol-fueled [63]. In an anode with a catalyst

layer, the partial oxidation of ethanol mainly took place in the catalyst layer first, and the anode catalyzed the oxidation of the products generated by the catalyst layer. With the help of the catalyst layer, the cell performance could be increased by partial pre-oxidation of ethanol. By adjusting the fabrication and the operating conditions of the cell, the PPD of the cell with a Cu/(ZnO-Al_2O_3) (40:30:30 wt% or 30:35:35 wt%) catalyst layer calcined at 1100 °C was ~50 mW/cm^2 in ethanol-air mixture fuel at 450 °C compared with 32 mW/cm^2 for a conventional cell under the same conditions. However, the instability of the cell performance, which was caused by the delamination and cracking at the interface during the re-oxidation of nickel, greatly undermined the prospects of Cu/(ZnO-Al_2O_3) catalyst layer in practical applications.

The above studies showed that the cell′s stability and electrochemical performance could be significantly improved with a copper-based catalyst layer. However, compared with the Ni-based catalyst layer, the Cu-based catalyst layer′s poor catalytic activity could result in a low conversion rate of the fuel when passing through the catalyst layer. The instability of the cell performance after long-term operation is still a critical problem, which could possibly be solved by improving the catalytic activity and the microstructure of the copper-based catalysts in the future.

3.1.4. Nickel-based alloy materials

The strong interaction between the 2p electrons of carbon and the 3d electrons of Ni is known as the main reason for the carbon deposition in Ni. A potential way to reduce coke formation over Ni is to alloy Ni with another metal such as Fe, Co, Cu, Sn,

and Au [17, 64-70], which can interact with the 3d electrons of Ni, thus improving the coking resistance of the nickel-based materials [71, 72]. Inspired by nickel-based alloy materials in the anode, and to mitigate the carbon deposition of the nickel-based catalyst layer, researchers have been exploring to apply Ni alloy as catalyst layer material, and promising results have been obtained. For example, Ni_xFe_y/ZrO_2 composite was used as catalyst layer material to improve the coking resistance of the Ni-YSZ anode in CH_4 fuel [73]. By optimizing Ni to Fe weight ratios in the catalysts, the Ni_4Fe_1/ZrO_2 catalysts were shown to possess slightly better coke resistance and lower graphitization degree than Ni/ZrO_2 catalysts in CH_4 fuel. A PPD of 1038 mW/cm^2 was obtained by the cell with a Ni_4Fe_1/ZrO_2 catalyst layer in CH_4/O_2 fuel at 850 °C, which is similar to that of the cell when H_2 was used as the fuel. To further improve the conductivity of the Ni_4Fe_1/ZrO_2 catalyst layer, the authors explored several methods to introduce 50 wt% Cu into the Ni_4Fe_1/ZrO_2 catalysts, and systematically investigated the effects on the catalytic activity for CH_4 conversion, coking resistance, and the cell performance. The studies showed that the catalysts prepared by the glycine-nitrate self-combustion method exhibited higher catalytic activity for the partial oxidation of CH_4 than the catalysts prepared by impregnation method and physical mixing method, however, the catalyst prepared by impregnation method possessed the highest coking resistance, and the cell with this catalyst layer prepared by impregnation method also exhibited attractive stability on CH_4/O_2 fuel for 100 h at 650 °C [74]. Lo Faro et al. [75] studied the catalytic activity of NiM/CGO (M = Cu or Co) composites as a catalyst layer for SOFCs. The ex-situ catalytic activity results indicated that both NiCu/CGO and

NiCo/CGO exhibited higher ethanol conversion than that of Ni/CGO. Moreover, the cell with NiCo/CGO showed better performance towards the direct utilization of dry ethanol than the conventional cell as well as with that using NiCu/CGO as the catalyst layer. A PPD of 550 mW/cm^2 was obtained by cell with NiCo/CGO catalyst layer in dry ethanol fuel at 800 °C. However, the authors did not compare the stability of the cell with and without a catalyst layer and thus further investigations are needed.

Studies on the formation of Ni-metal alloys through the incorporation of transition metals have been proved to be an effective method to enhance the coking tolerance of Ni-based anodes. In addition to the above-mentioned transition metals, there are some other candidates for increasing the coking tolerance, and the most promising of which is Sn. Sn has been added into SOFC anodes and exhibited good coking tolerance. Yoon et al. [76] prepared MNi (M: Ni = 1:3 atom %, M = Sn or Sb) catalysts by alloying Ni with Sn and Sb, respectively. Through reaction with water vapor, hydroxyl groups could be formed on the surface of Sn and Sb due to their hydrophilic properties, and carbon deposition on the metal surface could be effectively eliminated. Although the PPDs of the cells with SbNi/GDC and SnNi/GDC catalyst layers were ~15-20% lower than the conventional cells, the cells showed excellent stability during 200 h operation in CH_4 fuel at 650 °C without performance deterioration. The authors believed that the initial reduced cell performance could be explained by the barrier effect of the catalyst layer. For the cell with a catalyst layer, the catalyst layer can reduce the rate at which fuel can diffuse to the anode, thereby decreasing cell power density. Thus, exploring the optimal specific surface area and porosity of the catalyst layers will be an important direction

for the catalyst layer in future studies.

The stability of the cell with a nickel-based alloy catalyst layer could be improved in a short time. The formation of an alloy is a good strategy to enhance the coking resistance of the nickel-based catalysts. However, the metal ratio in the catalyst needs to be strictly controlled because the overall catalytic properties of nickel will be reduced after alloying with other metals [77]. Only by optimizing the composition of the nickel-based alloys can achieve the ideal cell performance. Thus, it is important to select metals that will form an alloy without decreasing the catalytic activity of the nickel catalyst. Moreover, to minimize performance loss caused by the addition of a catalyst layer and maintain the long-term operational stability, the micro-pore structure of the catalyst layer needs to be further optimized in the future.

3.1.5. Spinel-based materials

The general formula of spinel oxide materials is AB_2O_4. The valence state of A and B can be changed with the type and the molar ratio of A and B cations. Due to the adjustable and stable structure of the constituent elements, the studies on their catalytic activity have attracted much attention. In recent years, spinel oxides have been extensively proposed as catalysts for CH_4 reforming [78-81]. Jin et al. [82] pioneered the use of the spinel-based catalyst layer for SOFCs operating on CH_4 in 2010. The cell with a $Cu_{1.3}Mn_{1.7}O_4$-SDC (60:40 wt%) catalyst layer showed both high power outputs and considerable stability in CH_4 fuel at 650 °C for about 60 h. In comparison, the cell without the catalyst layer was deactivated quickly and failed after 16 h of operation.

The authors believed that the good stability of MnO and the strong interaction between MnO and Cu could contribute to the excellent catalytic activity for CH_4 steam reforming. After the spinel was reduced, well-dispersed fine Cu metallic particles with high specific surface area in the MnO matrix would be formed, which could effectively accelerate CH_4 steam reforming to produce H_2 and CO. The formed H_2 and CO will then diffuse to the anode active layer. Thus, the cell with a $Cu_{1.3}Mn_{1.7}O_4$ exhibited considerably stable performance in CH_4 fuel.

Besides the $Cu_{1.3}Mn_{1.7}O_4$ as catalyst layer materials in SOFCs, Ni-based spinel and Fe-based spinel catalysts have also been demonstrated to be the active catalyst layer materials for SOFCs operating on CH_4. Hua et al. [83] used $MnNi_2O_4$ synthesized by a sol-gel method as the catalyst layer material and deposited directly on the anode by screen printing. The Ni-MnO composite reduced from $MnNi_2O_4$ can be used as an effective catalyst for CH_4 reforming. The electrochemical performance was evaluated through the three-electrode method. With the help of this catalyst layer, open circuit polarization resistance of the anode decreased by approximately more than 1/3 compared with the conventional anode in wet CH_4 within all test temperature ranges. Although the anode with this catalyst layer could not completely avoid carbon deposition during long-time operation, the anode showed higher coking resistance at open circuit than the conventional one. Moreover, the formed carbon in the anode with this catalyst layer exhibited a lower degree of graphitization, and the carbon deposition could be prevented with the addition of 20% H_2O at 800 °C and 200 mA/cm^2. The reduced $MnNi_2O_4$ catalyst layer can convert the CH_4-20 mol%H_2O mixing gas into H_2

and CO before it diffused into the anode. However, the addition of high H_2O content may reduce the concentration of the fuel, thereby affecting the working efficiency of the cells. $Ni_{0.5}Cu_{0.5}Fe_2O_4$ (NCFO) spinel was also prepared as catalyst layer materials. Under a reducing atmosphere, the NCFO was totally reduced into metallic Ni-Fe and Cu-Fe alloys. Those alloys exhibited high catalytic activity for the oxidation of CH_4. As the coefficient of thermal expansion (CTE) of the reduced NCFO is higher than that of the initial spinel, GDC was used to modify the CTE of the catalyst layer to match that of the cell. With the help of the NCFO-GDC catalyst layer, open circuit polarization resistance of the anode decreased to 1/2 in wet CH_4 of that of the conventional anode in all test temperature ranges. During the test at 800 °C and 200 mA/cm^2, carbon deposition could be prevented when H_2O content reached or exceeded 7 mol% in the fuel compared with that of the $MnNi_2O_4$ catalyst layer [84]. To further improve coking resistance of the anode, a $Ni_{0.5}Cu_{0.5}Fe_2O_4$-$BaZr_{0.1}Ce_{0.7}Y_{0.1}Yb_{0.1}O_{3-\delta}$ (NCF-BZCYYb) composite as catalyst layer material was invested in CH_4 fuel. Compared with GDC, BZCYYb could effectively promote CH_4 reforming and carbon removal reactions due to its strong ability to store H_2O and adsorb CO_2. The formed carbon could be effectively removed in the anode by adding only 3 mol% H_2O into dry CH_4 [85]. The performance of the cell with an NCF-BZCYYb catalyst layer in the fuel of CH_4/33.3 mol% H_2O was considerably enhanced above the level of the conventional one, demonstrating a PPD of 1638 mW/cm^2 and a stable power density of 485 mW/cm^2 at 800 °C for 48 h without carbon formation (Fig. 7) [86].

$MnFe_2O_4$ as the catalyst layer material was investigated for SOFCs operating on

bio-syngas [87]. Cells with and without a $MnFe_2O_4$ catalyst layer were tested in simulated bio-syngas at 750 °C. Although the deterioration of the cell′s performance was observed under operation with a $MnFe_2O_4$ catalyst layer, the cell′s coking resistance was greatly improved and the best performance was obtained when the $MnFe_2O_4$ was added with 16 wt% graphite. The authors believed that the following three factors improved the excellent coking resistance of the cell: (1) the catalyst layer could serve as a diffusion barrier layer to reduce the direct contact between the anode and fuel gas; (2) the reduced $MnFe_2O_4$ could convert the simulated biosygas into other gases such as H_2 and CO_2; and (3) the catalyst layer changed the partial pressure of various gases inside the anode, thus preventing the anode from carbon deposition.

In addition to the Ni and Fe-based spinel catalyst materials in SOFCs, Zhao et al. [88] reported a MnO-Co composite catalyst layer formed by in-situ reduction of $Mn_{1.5}Co_{1.5}O_4$ spinel. Co was an active catalyst for CH_4 reforming. It could absorb and activate molecule water as the form of hydroxyl groups. MnO acted as an excellent promoter for CH_4 reforming and carbon suppression. The MnO-Co composite catalyst layer could pre-reform CH_4 into syngas and suppress the carbon deposition, and therefore improved the stability of the SOFCs with MnO-Co-containing catalyst layers. Although the durability of cells with a $Mn_{1.5}Co_{1.5}O_4$ catalyst layer was enhanced in wet CH_4, the addition of the catalyst layer reduced the electrochemical performance of the cell because of the increase in mass transport resistance. To solve the above problem, SDC promoters were added to this catalyst layer. SDC could increase the porosity of the catalyst and facilitate gas diffusion, as shown in Fig.8 (a & b). With the help of SDC

promoters, the PPD of the cell with a $Mn_{1.5}Co_{1.5}O_4$-SDC catalyst layer was increased by 12.3% compared with the conventional cell in wet CH_4 at 650 °C, and the cell also operated stably for 360 min without degradation (Fig. 8(c)). The authors illustrated the schematic diagram of the cell with a $Mn_{1.5}Co_{1.5}O_4$ catalyst layer. According to their description (Fig. 8(d)), wet CH_4 could be effectively converted into syngas by this catalyst layer before reaching the anode side, improving the stability and electrochemical performance of the cell with this catalyst layer.

The high conductivity of the spinel-based materials after reduction can solve the problem of the current collection in the cell with a catalyst layer. However, as the CTE of the reduced spinel is higher than that of the initial one, which causes instability of the cell at high operating temperatures. Adjusting the CTE value of spinel-based materials to match well with the anode can be the future direction that requires further investigation. In addition to compositing the spinel-based materials with electrolyte material [84], a recent report of an ideal thermal matching between cathodes and electrolytes could be obtained by adding a negative thermal expansion oxide into the cathode was proven to be an effective strategy to reduce the CTE value of electrodes without imposing negative effects [89]. It is possible to adjust the overall CTE of the spinel-based catalyst layer by compositing spinel-based materials with appropriately chosen materials with different thermal expansion behaviors.

3.1.6. Perovskite-based materials

Perovskite type oxides with the chemical formula of ABO_3 were investigated as

catalysts in SOFCs by various groups due to their excellent thermal and mechanical stability, physical compatibility with typical electrolytes, coking resistance and low cost [90]. Good stability of the cell performance can be achieved by combining traditional anode materials with high catalytic activity and perovskite materials with excellent coking resistance. The perovskite oxides used as catalyst layer can be simply divided into redox stable materials and redox unstable materials. The redox stable perovskite oxides are usually derived from traditional anode materials, which can maintain their structure unchanged in a reducing atmosphere. For instance, Huang et al. [91] used $La_{0.75}Sr_{0.25}Cr_{0.5}Mn_{0.5}O_3$-$CeO_2$ (LSCM-CeO_2) as the catalyst layer in SOFCs operating on ethanol. The CeO_2 exhibited high electrocatalytic activity for hydrocarbon oxidation, which could reform the ethanol before it can reach the anode. Moreover, LSCM as a p-type conductor provided the conductivity and connectivity path of the anode system. For the cell with the LSCM-CeO_2 catalyst layer, the ethanol steam reforming took place in the catalyst layer first, and then the supported anode catalyzed the oxidation of the products. By optimizing the fabrication condition and the LSCM to CeO_2 ratio, cells with the LSCM-CeO_2 (with weight ratio 1:3) catalyst layer calcined at 1100 °C generated an attractive PPD of 669 mW/cm^2 at 850 °C operating on ethanol fuel. The cell also showed excellent stability for 216 h on ethanol fuel at 700 °C.

Different from the redox stable perovskite oxides, the redox unstable perovskite oxides are usually reduced into oxides and metal particles in a reducing atmosphere. $NiTiO_3$ (NTO) catalyst layer was used by Wang et al. [92] to enhance the coking resistance of nickel-based anodes. Under a reducing atmosphere, NTO was reduced to

TiO_2 and metallic Ni, which could efficiently accelerate the CH_4 steam reforming reaction and decrease CH_4 cracking in the anode by reforming CH_4 into syngas. Cells with the NTO catalyst layer generated a PPD of 236 mW/cm^2 at 700 °C when operated on wet CH_4, while the PPD of the conventional cell was 146 mW/cm^2 under the same condition. Moreover, cells with this catalyst layer also showed excellent operational durability on propane fuel for 26 h at 700 °C, while the conventional cell failed within 1 h. For cells with the $La_{0.6}Sr_{0.4}Co_{0.2}Fe_{0.8}O_3$ (LSCF) catalyst layer, reasonable stability was maintained for 475 h in the reducing environment under CH_4 flow at 750 °C, whereas cells without a catalyst layer failed after being operated for only 38 h. The reduced LSCF showed high catalytic activity toward CH_4 or carbon with O^{2-} anions transported from YSZ to release electrons produced during the reaction to the Ni connected particles. Since oxygen ions could be oxidized into oxygen molecules on LSCF at the operating temperature of SOFCs, the oxidation reaction of CH_4 and carbon deposits could be accelerated with the formation of oxygen molecules. This could slow down the degradation of the anode. It was found that the LSCF still maintained its perovskite structure after the long-term stability test. The authors believed that LSCF might undergo a decomposition/re-oxidation process due to the increase in the crystallite size of LSCF after the long-term stability test. However, the mechanism of the re-oxidation process of LSCF was unclear, and thus requiring further investigation [93]. Lv et al. [94] found that $La_{0.7}Sr_{0.3}Fe_{0.8}Ni_{0.2}O_{3-\delta}$ (LSFN) could be reduced with the formation of $Fe_{0.64}Ni_{0.36}$, $SrLaFeO_4$, and La_2O_3 under a reducing atmosphere. The Fe-Ni alloy could decrease CH_4 cracking by reforming CH_4 into syngas. The CH_4

conversion over the reduced catalyst reached 98.24 % at 900 °C, which was nearly 2.7 times higher than that without the catalyst (36.83%). Loading the catalyst onto a Ni-YSZ anode would likely improve the coking resistance when using CH_4-based fuels. Compared with the conventional cells, the PPDs of the cells with this catalyst layer increased by 26.01% and 24.48% at 850 °C when operated on 97% CH_4/3 % H_2O and 30% CH_4/70% air fuels, respectively. Moreover, when fed with CH_4/H_2O and CH_4/air, cells with these catalyst layers were stable for at least 110 h and 120 h, respectively (Fig. 9).

Although the combination of perovskite materials and traditional anode materials can effectively alleviate carbon deposition of the anode, perovskite materials exhibit poor catalytic activity for hydrocarbon-based fuel. In addition, perovskite-type oxides possess relatively low conductivity under a reducing atmosphere, which requires a solution to the current collection for cells in practical application [93]. Enhancing the catalytic activity and the conductivity of the perovskite-based catalyst layer can be the future direction to be explored in depth. In recent years, perovskites oxides with metal or alloy nanoparticle exsolution have been extensively investigated due to their higher electrocatalytic activities [45, 46, 95, 96]. The nanoparticle exsolution from the perovskite bulk has been extensively reported, such as $Sm_{0.8}Sr_{0.2}Fe_{0.8}Ti_{0.15}Ru_{0.05}O_{3-\delta}$ [97], $Sr_2FeMo_{0.65}Ni_{0.35}O_{6-\delta}$ [95], $Pr_{0.4}Sr_{0.6}Co_{0.2}Fe_{0.7}Nb_{0.1}O_{3-\delta}$ [98] and $Sr_2Fe_{1.3}Co_{0.2}Mo_{0.5}O_{6-\delta}$ [99]. These exsolved nanoparticles were well-dispersed and provide active sites for fuel oxidation, which exhibited higher stability than these nanoparticles prepared by the infiltration method during the high temperature operating

process. Moreover, the conductivity of perovskite could also be increased due to the exsolved alloy phase [100]. Due to the high activity of the dispersed metallic nanoparticles supported on the bulk perovskite oxide matrix, the catalytic activity and the conductivity of the perovskite-based catalyst layer can be further improved.

3.1.7. Other types of materials

Besides the aforementioned catalyst layer materials, some other oxides have also been used for catalyst layers and achieved good results. Suzuki et al. [101] utilized CeO_2 as the catalyst layer and successfully reduced the operating temperature of a single cell to 449 °C. Since the CeO_2 catalysts showed catalytic activity for reforming reactions, the carbonaceous fuels would be reformed to syngas when passing through the catalyst layer. Then the syngas flowing to the anode for the electrochemical reactions, which could facilitate the electrochemical oxidation of the fuels at the anode and enhanced the performance of the cell. A PPD of approximately 110 mW/cm^2 was obtained by cells with CeO_2 catalyst layer in CH_4/H_2O fuel at 449 °C, while the power output of the conventional cell was suddenly dropped due to the falloff in the catalytic activity of the anode under the same condition. Recently, Wang et al. [102] used $Ce_{0.8}Ni_{0.2}O_{2-\delta}$ (CNO) to suppress the carbon deposition in SOFCs operating on wet CH_4. They found that part of Ni species was highly dispersed over CNO, and the others were incorporated into the CeO_2 lattice. In a reducing atmosphere, the Ni^{2+} dopants exhibited good stability, while the dispersed Ni species were reduced to metallic Ni. The authors believed that the CNO could exhibit high catalytic activity for CH_4 reforming due to

the metallic Ni formed in the CNO and surface oxygen vacancies generated with the doping of Ni^{2+} into the CeO_2 lattice. For the cells with this catalyst layer, CH_4 should first pass through the catalyst layer before reaching the anode. In this way, the concentration of the CH_4 inside the anode layer was minimized and coking on the anode was avoided. PPD of 664 mW/cm^2 was obtained for the cell with a CNO catalyst layer operating on wet CH_4 at 650 °C, and the cell operated stably for 40 h without performance deterioration or carbon formation, whereas the voltage of the conventional cell was reduced by 43.1% after ~26 h of operation. The result indicated that the cell with the CNO catalyst layer showed both improved performance and stability in wet CH_4. Yuan et al. [103] coated CeO_2-BaO-NiO composite oxide with SiO_2 to prepare CeO_2-BaO-NiO@SiO_2 catalyst with core-shell structure (@NBC). The CeO_2-BaO-NiO showed high catalytic activity toward CH_4 partial oxidation, CO_2 and steam reforming. Meanwhile, the confinement effect of a porous inert shell prevented Ni particles from sintering which could provide more active sites for CH_4 partial oxidation/reforming during longtime operation. The cell without a catalyst layer yielded a PPD of 625 mW/cm^2 at 800 °C when operated on CH_4/air fuel, whereas the performance of the cell with a @NBC catalyst layer was improved, with a PPD of 938 mW/cm^2 under the same conditions. Moreover, they compared the effect of CeO_2-BaO-NiO without core-shell structure (NBC) on the stability of the cell. The study found that the cell with @NBC showed excellent stability with a 0.005 V/h average degradation rate within 163 h, whereas the cell with NBC was dramatically failed after 10 h of operation under the same conditions. Performances of hydrocarbon-fueled SOFCs with a directly-loaded

catalyst layer are summarized in Table 1. The cells with a catalyst layer show excellent stability and reasonable power outputs.

3.2. The independent catalyst layer

Depositing a catalyst layer on the anode surface directly can be a good solution to improve the performance and stability of the cell. However, this preparation method may cause small catalyst particles inevitably infiltrate into the pores of the anode and influence the fuel diffusion. It can also lead to the cell cracking and obvious delamination of the catalyst layer due to the mismatch of TECs between the catalyst layer and the anode. Moreover, the reforming reaction of hydrocarbons requires high activation energy and causes local temperature variation across the anode, which may lead to cell cracking [104, 105]. Therefore, some researchers designed an independent catalyst layer, as shown in Fig. 3. The separation of the catalyst layer from the cell not only enables the fuel to be converted before diffusing to the anode, but also avoids the problems caused by the direct deposition of the catalyst layer. For instance, Chang et al. [106] prepared a double-layered catalyst slice which was composed of a $La_{0.6}Sr_{0.4}Co_{0.2}Fe_{0.8}O_{3-\delta}$ (LSCF) catalyst layer and an Al_2O_3 substrate layer. Under a reducing atmosphere, a K_2NiF_4-type oxide (Sr, La) FeO_4 and highly dispersed Co-Fe alloy could be achieved from LSCF, which exhibited excellent catalytic activity for CH_4 partial oxidation with 88% conversion at 950 °C in a mixture of CH_4 and O_2 (1: 1). With the help of this independent catalyst layer, the voltage of the cell stabilized at 0.79 V with negligible degradation within 116 h compared to the conventional cell, which

failed within 20 min when operated on wet CH_4 as fuel at 800 °C. After the stability test, the conventional cell showed many cracks, while the cell with the LSCF catalyst layer remained intact after 116 h of operation. Moreover, they also used $La_{0.7}Sr_{0.3}Cr_{0.8}Fe_{0.2}O_{3-\delta}$ [107] and $Sr_2MoFeO_{6-\delta}$ [108] as independent catalyst layers, respectively. They are both well-known anode materials in SOFCs which exhibit good catalytic activity for hydrocarbon-based fuel. The cells exhibited favorable stability for 100 h and 55 h on wet CH_4 at 800 °C, respectively, while the conventional cells decayed rapidly in approximately 30 min and 20 min under the same conditions.

Besides the perovskite-based catalysts, metal oxide composite catalysts are also demonstrated to be the active anode independent catalyst layer materials for SOFCs operating on carbonaceous fuel. For example, Zhao et al. [109] applied the NiMo/CeO_2-ZrO_2 catalyst on both surfaces of the porous YSZ substrate and used it as an independent catalyst layer for Ni-YSZ anode supported cells. For the cell with this catalyst layer, complex isooctane fuels would be reformed to syngas in the catalytic reforming layer, and the reformed gas would be delivered to the anode for the electrochemical reactions, which could facilitate the electrochemical oxidation of complex hydrocarbons at the anode and enhanced the coking resistance of it. Compared with the conventional cell, the cell with an independent catalyst layer showed excellent stability with a 3.0 mV/h average degradation during a 12 h stability test at 750 °C. After the stability test, carbon amount of the anode with an independent catalytic layer (8 wt%) was found to be significantly less than that of the conventional cell (26 wt%), as shown in Fig. 10. The results indicated the effectiveness of the independent catalyst layer for suppressing

carbon deposition and improving the cell′s performance in isooctane/air. NiO-BaO-CeO_2 as the independent catalyst layer material was also used by Chen et al. [110] to suppress coke formation in SOFCs operating with low concentration coal-bed-gas (LC-CBG: 30% CH_4/70% air). This Ni-based catalysts showed a superior catalytic activity for CH_4 partial oxidation, CH_4 steam reforming and CH_4 dry reforming. Since the electrochemical activity of CO and H_2 achieved from CH_4 partial oxidation/reforming was higher than that of CH_4, the cells′ performance with a catalyst layer was higher than that of the conventional one. PPD of cells with an independent catalytic layer increased by approximately 41.9% compared with the conventional cell at 800 °C. The cell also showed good stability for 55 h on LC-CBG fuel, whereas the conventional cell decayed rapidly after 4 h of operation under the same conditions.

Performances of SOFCs with an independent catalyst layer are summarized in Table 2. Although the coking resistance of the cell is significantly improved with the independent catalyst layer in hydrocarbon fuels, the sealing process of the cell is relatively complicated. The study about the long-term stability of the cell with the independent catalyst layer still lacks, and the assembly design of the independent catalyst layer in the cell stacks requires further investigation.

4 Conclusions and perspectives

SOFCs can directly operate using hydrocarbon-based fuel, however, coking is a pressing issue with the traditional Ni-cermet SOFC anode. Utilization of catalyst layers in the SOFC anode can significantly improve the electrochemical performance and

coking resistance operating with hydrocarbon-based fuel. Recent progress in the catalyst layer employed in traditional Ni-cermet SOFC anode is comprehensively reviewed. The advantages and limitations, as well as further enhancement needs have been summarized for the direct-loaded and independent catalyst layers employed for the conventional Ni-cermet SOFC anode. The following directions for the SOFC anode catalyst layer can be explored in-depth in the future in order to enhance the cell performance and mitigate carbon deposition for Ni-cermet anodes directly using hydrocarbon fuels: (1) enhancing the catalytic activity and the coking resistance of the catalyst layer materials for hydrocarbon-based fuel; (2) exploring the optimal specific surface area and porosity of the catalyst layers; (3) adjusting the thermal expansion coefficient of the catalyst layers to better match with other cell components; (4) improving the electrical conductivity of the catalyst layers, and incorporating the current collection in the catalyst layers; (5) studying the assembly and implementation of the independent catalyst layer in a cell stack; and (6) understanding the mechanism of the catalyst layers by combining experimental studies with modeling and simulations.

Acknowledgments

This work was financially supported by National Key Research and Development Program of China (2018YFE0106700), National Natural Science Foundation of China (52072405), the U.S. National Science Foundation (DMR-1832809) and the Yueqi Young Scholar Project (CUMTB).

Reference

[1] Diaz-Saldierna LH, Leyva-Ramos J, Langarica-Cordoba D, Ortiz-Lopez MG. Energy processing from fuel-cell systems using a high-gain power dc-dc converter: Analysis, design, and implementation. Int J Hydrogen Energy 2021;46:25264-76.

[2] Liu M, Lynch ME, Blinn K, Alamgir FM, Choi Y. Rational SOFC material design: new advances and tools. Materials Today 2011;14:534-46.

[3] Sarruf BJM, Hong J-E, Steinberger-Wilckens R, de Miranda PEV. Ceria-Co-Cu-based SOFC anode for direct utilisation of methane or ethanol as fuels. Int J Hydrogen Energy 2020;45:5297-308.

[4] Zendrini M, Testi M, Trini M, Daniele P, Van Herle J, Crema L. Assessment of ammonia as energy carrier in the use with reversible solid oxide cells. Int J Hydrogen Energy 2021;46:30112-23.

[5] Miyazaki K, Okanishi T, Muroyama H, Matsui T, Eguchi K. Development of Ni-$Ba(Zr,Y)O_3$ cermet anodes for direct ammonia-fueled solid oxide fuel cells. J Power Sources 2017;365:148-54.

[6] Stoeckl B, Subotić V, Reichholf D, Schroettner H, Hochenauer C. Extensive analysis of large planar SOFC: Operation with humidified methane and carbon monoxide to examine carbon deposition based degradation. Electrochim Acta 2017;256:325-36.

[7] Yu F, Han T, Wang Z, Xie Y, Wu Y, Jin Y, et al. Recent progress in direct carbon solid oxide fuel cell: Advanced anode catalysts, diversified carbon fuels, and heat

management. Int J Hydrogen Energy 2021;46:4283-300.

[8] Xie Y, Lu Z, Ma C, Xu Z, Tang Y, Ouyang S, et al. High-performance gas-electricity cogeneration using a direct carbon solid oxide fuel cell fueled by biochar derived from camellia oleifera shells. Int J Hydrogen Energy 2020;45:29322-30.

[9] Singh M, Zappa D, Comini E. Solid oxide fuel cell: Decade of progress, future perspectives and challenges. Int J Hydrogen Energy 2021;46:27643-74.

[10] Chan SH. A review of anode materials development in solid oxide fuel cells. J Mater Sci 2004;39:4405-39.

[11] Ge XM, Chan SH, Liu QL, Sun Q. Solid Oxide Fuel Cell Anode Materials for Direct Hydrocarbon Utilization. Advanced Energy Materials 2012;2:1156-81.

[12] Shri Prakash B, Senthil Kumar S, Aruna ST. Properties and development of Ni/YSZ as an anode material in solid oxide fuel cell: A review. Renewable and Sustainable Energy Reviews 2014;36:149-79.

[13] He H, Hill JM. Carbon deposition on Ni/YSZ composites exposed to humidified methane. Applied Catalysis A: General 2007;317:284-92.

[14] Koh JH, Yoo YS, Park JW, Lim HC. Carbon deposition and cell performance of Ni-YSZ anode support SOFC with methane fuel. Solid State Ionics 2002;149:157-66.

[15] Timmermann H, Fouquet D, Weber A, Ivers-Tiffée E, Hennings U, Reimert R. Internal Reforming of Methane at Ni/YSZ and Ni/CGO SOFC Cermet Anodes. Fuel Cells 2006;6:307-13.

[16] Prasad DH, Park SY, Ji H, Kim HR, Son JW, Kim BK, et al. Effect of steam content

on nickel nano-particle sintering and methane reforming activity of Ni-CZO anode cermets for internal reforming SOFCs. Applied Catalysis A: General 2012;411-412:160-9.

[17] Niakolas DK, Ouweltjes JP, Rietveld G, Dracopoulos V, Neophytides SG. Au-doped Ni/GDC as a new anode for SOFCs operating under rich CH_4 internal steam reforming. Int J Hydrogen Energy 2010;35:7898-904.

[18] Chen XJ, Khor KA, Chan SH. Suppression of Carbon Deposition at CeO_2-Modified Ni/YSZ Anodes in Weakly Humidified CH_4 at 850 °C. Electrochem Solid-State Lett 2005;8:79-82.

[19] Cimenti M, Hill JM. Direct utilization of ethanol on ceria-based anodes for solid oxide fuel cells. Asia-Pac J Chem Eng 2009;4:45-54.

[20] Tao S, Irvine JT, Plint SM. Methane oxidation at redox stable fuel cell electrode $La_{0.75}Sr_{0.25}Cr_{0.5}Mn_{0.5}O_{3-\delta}$. The Journal of Physical Chemistry B 2006;110:21771-6.

[21] Yang C, Yang Z, Jin C, Xiao G, Chen F, Han M. Sulfur-tolerant redox-reversible anode material for direct hydrocarbon solid oxide fuel cells. Adv Mater 2012;24:1439-43.

[22] Wei K, Wang X, Budiman RA, Kang J, Lin B, Zhou F, et al. Progress in Ni-based anode materials for direct hydrocarbon solid oxide fuel cells. J Mater Sci 2018;53:8747-65.

[23] Jung S, Lu C, He H, Ahn K, Gorte RJ, Vohs JM. Influence of composition and Cu impregnation method on the performance of Cu/CeO_2/YSZ SOFC anodes. J Power Sources 2006;154:42-50.

[24] Gorte RJ, Park S, Vohs JM, Wang C. Anodes for direct oxidation of dry hydrocarbons in a solid-oxide fuel cell. Adv Mater 2000;12:1465-9.

[25] Qiu P, Sun S, Yang X, Chen F, Xiong C, Jia L, et al. A review on anode on-cell catalyst reforming layer for direct methane solid oxide fuel cells. Int J Hydrogen Energy 2021;46:25208-24.

[26] Zhan Z, Barnett SA. An octane-fueled solid oxide fuel cell. Science 2005;308:844-7.

[27] Gür TM. Comprehensive review of methane conversion in solid oxide fuel cells: Prospects for efficient electricity generation from natural gas. Progr Energy Combust Sci 2016;54:1-64.

[28] Lin Y, Zhan Z, Barnett SA. Improving the stability of direct-methane solid oxide fuel cells using anode barrier layers. J Power Sources 2006;158:1313-6.

[29] Barison S, Fabrizio M, Mortalò C, Antonucci P, Modafferi V, Gerbasi R. Novel Ru/$La_{0.75}Sr_{0.25}Cr_{0.5}Mn_{0.5}O_{3-\delta}$ catalysts for propane reforming in IT-SOFCs. Solid State Ionics 2010;181:285-91.

[30] Monteiro NK, Candido GAS, Fonseca FC. Synthesis of Ru-doped Double Perovskite Anode for SOFC. ECS Trans 2017;78:1245-52.

[31] Su C, Wang W, Liu M, Tadé MO, Shao Z. Progress and Prospects in Symmetrical Solid Oxide Fuel Cells with Two Identical Electrodes. Advanced Energy Materials 2015;5:1-19.

[32] Sugimoto J, Futamura S, Kawabata T, Lyth SM, Shiratori Y, Taniguchi S, et al. Ru-based SOFC anodes: Preparation, performance, and durability. Int J Hydrogen

Energy 2017;42:6950-64.

[33] Zhan Z, Barnett SA. Operation of ceria-electrolyte solid oxide fuel cells on iso-octane-air fuel mixtures. J Power Sources 2006;157:422-9.

[34] Zhan Z, Barnett SA. Solid oxide fuel cells operated by internal partial oxidation reforming of iso-octane. J Power Sources 2006;155:353-7.

[35] Liu X, Zhan Z, Meng X, Huang W, Wang S, Wen T. Enabling catalysis of Ru-CeO_2 for propane oxidation in low temperature solid oxide fuel cells. J Power Sources 2012;199:138-41.

[36] Wang W, Ran R, Shao Z. Combustion-synthesized Ru-Al_2O_3 composites as anode catalyst layer of a solid oxide fuel cell operating on methane. Int J Hydrogen Energy 2011;36:755-64.

[37] Sun C, Xie Z, Xia C, Li H, Chen L. Investigations of mesoporous CeO_2-Ru as a reforming catalyst layer for solid oxide fuel cells. Electrochem Commun 2006;8:833-8.

[38] Wang K, Ran R, Shao Z. Methane-fueled IT-SOFCs with facile in situ inorganic templating synthesized mesoporous $Sm_{0.2}Ce_{0.8}O_{1.9}$ as catalytic layer. J Power Sources 2007;170:251-8.

[39] Nóbrega SD, Steil M, Georges S, Uhlenbruck S, Fonseca FC. Direct ethanol anode-supported solid oxide fuel cell. ECS Trans 2015;68:2851-8.

[40] Sun L, Liu L, Luo L, Wu Y, Shi J, Cheng L, et al. Facile synthesis of flower-like Pd catalyst for direct ethanol solid oxide fuel cell. Journal of Fuel Chemistry and Technology 2016;44:607-12.

[41] Song S, Wang X, Zhang H, CeO_2-Encapsulated Noble Metal Nanocatalysts: Enhanced Activity and Stability for Catalytic Application, NPG Asia Mater. 2015;7:179-97.

[42] Zhang C, Li S, Wang T, Wu G, Ma X, Gong J, Pt-based core-shell nanocatalysts with enhanced activity and stability for CO oxidation, Chem. Commun. 2013;49: 10647-9.

[43] Qin M, Tan T, Li K, Wang Z, Yang H, Liu Z, et al. In-situ exsolved FeRu alloy nanoparticles on Ruddlesden-Popper oxides for direct hydrocarbon fuel solid oxide fuel cells. Int J Hydrogen Energy 2020;45:21464-72.

[44] He S, Li M, Hui J, Yue X. In-situ construction of ceria-metal/titanate heterostructure with controllable architectures for efficient fuel electrochemical conversion. Applied Catalysis B: Environmental 2021;298:120588-600.

[45] Qin M, Xiao Y, Yang H, Tan T, Wang Z, Fan X, et al. Ru/Nb co-doped perovskite anode: Achieving good coking resistance in hydrocarbon fuels via core-shell nanocatalysts exsolution. Applied Catalysis B: Environmental 2021;299:120613-21.

[46] Thommy L, Benamira M, Jardiel T, Günes V, Joubert O, Caldes MT. Ru exsolution in substituted $La_{0.75}Sr_{0.25}Cr_{0.5}Mn_{0.5}O_{3-\delta}$ compound as anode material for an IT-SOFCs. Mater Chem Phys 2021;268:124724-34.

[47] Wang D, Wong SI, Sunarso J, Xu M, Wang W, Ran R, et al. A Direct n-Butane Solid Oxide Fuel Cell Using $Ba(Zr_{0.1}Ce_{0.7}Y_{0.1}Yb_{0.1})_{0.9}Ni_{0.05}Ru_{0.05}O_{3-\delta}$ Perovskite as the Reforming Layer. ACS Appl Mater Interfaces 2021;13:20105-13.

[48] Wang W, Zhou W, Ran R, Cai R, Shao Z. Methane-fueled SOFC with traditional nickel-based anode by applying Ni/Al_2O_3 as a dual-functional layer. Electrochem Commun 2009;11:194-7.

[49] Wang RP, Mao SH, Duan XQ, Lin WB, Wang Q, Chi YQ. Catalytic performance of nickel-based catalysts with different supports in partial oxidation of methane to synthesis gas. Ranliao Huaxue Xuebao/Journal of Fuel Chemistry and Technology 2015;43:228-34.

[50] Zhang G, Liu J, Xu Y, Sun Y. A review of CH_4-CO_2 reforming to synthesis gas over Ni-based catalysts in recent years (2010-2017). Int J Hydrogen Energy 2018;43:15030-54.

[51] Wang W, Ran R, Shao Z. Lithium and lanthanum promoted Ni-Al_2O_3 as an active and highly coking resistant catalyst layer for solid-oxide fuel cells operating on methane. J Power Sources 2011;196:90-7.

[52] Wang W, Wang F, Chen Y, Qu J, Tade MO, Shao Z. Ceramic Lithium Ion Conductor to Solve the Anode Coking Problem of Practical Solid Oxide Fuel Cells. ChemSusChem 2015;8:2978-86.

[53] Wang W, Su C, Ran R, Park HJ, Kwak C, Shao Z. Physically mixed LiLaNi-Al_2O_3 and copper as conductive anode catalysts in a solid oxide fuel cell for methane internal reforming and partial oxidation. Int J Hydrogen Energy 2011;36:5632-43.

[54] Zhao J, Xu X, Zhou W, Blakey I, Liu S, Zhu Z. Proton-Conducting La-Doped Ceria-Based Internal Reforming Layer for Direct Methane Solid Oxide Fuel Cells. ACS Appl Mater Interfaces 2017;9:33758-65.

[55] Simwonis D, Tietz F, Stöver D. Nickel coarsening in annealed Ni/8YSZ anode substrates for solid oxide fuel cells. Solid State Ionics 2000;132:241-51.

[56] Lee JH, Moon H, Lee HW, Kim J, Kim JD, Yoon KH. Quantitative analysis of microstructure and its related electrical property of SOFC anode, Ni-YSZ cermet. Solid State Ionics 2002;148:15-26.

[57] Goula MA, Charisiou ND, Papageridis KN, Delimitis A, Pachatouridou E, Iliopoulou EF. Nickel on alumina catalysts for the production of hydrogen rich mixtures via the biogas dry reforming reaction: Influence of the synthesis method. Int J Hydrogen Energy 2015;40:9183-200.

[58] Taherian Z, Khataee A, Orooji Y. Nickel-based nanocatalysts promoted over MgO-modified SBA-16 for dry reforming of methane for syngas production: Impact of support and promoters. J Energy Inst 2021;97:100-8.

[59] Laosiripojana N, Assabumrungrat S. Catalytic steam reforming of ethanol over high surface area CeO_2: The role of CeO_2 as an internal pre-reforming catalyst. Applied Catalysis B: Environmental 2006;66:29-39.

[60] Ye XF, Wang SR, Wang ZR, Xiong L, Sun XF, Wen TL. Use of a catalyst layer for anode-supported SOFCs running on ethanol fuel. J Power Sources 2008;177:419-25.

[61] Ye XF, Wang SR, Hu Q, Wang ZR, Wen TL, Wen ZY. Improvement of multi-layer anode for direct ethanol Solid Oxide Fuel Cells. Electrochem Commun 2009;11:823-6.

[62] Ye XF, Wang SR, Zhou J, Zeng FR, Nie HW, Wen TL. Application of a Cu-

CeO_2/Ni-yttria-stabilized zirconia multi-layer anode for anode-supported Solid Oxide Fuel Cells operating on H_2-CO syngas fuels. J Power Sources 2011;196:5499-502.

[63] Morales M, Espiell F, Segarra M. Improvement of performance in low temperature solid oxide fuel cells operated on ethanol and air mixtures using Cu-ZnO-Al_2O_3 catalyst layer. J Power Sources 2015;293:366-72.

[64] Kan H, Lee H. Enhanced stability of Ni-Fe/GDC solid oxide fuel cell anodes for dry methane fuel. Catal Commun 2010;12:36-9.

[65] Tsai HC, Morozov SI, Yu TH, Merinov BV, Goddard WA. First-Principles Modeling of Ni_4M (M = Co, Fe, and Mn) Alloys as Solid Oxide Fuel Cell Anode Catalyst for Methane Reforming. The Journal of Physical Chemistry C 2015;120:207-14.

[66] Kim H, Lu C, Worrell WL, Vohs JM, Gorte RJ. Cu-Ni Cermet Anodes for Direct Oxidation of Methane in Solid-Oxide Fuel Cells. J Electrochem Soc 2002;149:247-50.

[67] Nikolla E, Schwank J, Linic S. Promotion of the long-term stability of reforming Ni catalysts by surface alloying. J Catal 2007;250:85-93.

[68] Nikolla E, Schwank J, Linic S. Hydrocarbon steam reforming on Ni alloys at solid oxide fuel cell operating conditions. Catal Today 2008;136:243-8.

[69] Myung Jh, Kim SD, Shin TH, Lee D, Irvine JTS, Moon J, et al. Nano-composite structural Ni-Sn alloy anodes for high performance and durability of direct methane-fueled SOFCs. Journal of Materials Chemistry A 2015;3:13801-6.

[70] Wu H, La Parola V, Pantaleo G, Puleo F, Venezia A, Liotta L. Ni-Based Catalysts for Low Temperature Methane Steam Reforming: Recent Results on Ni-Au and Comparison with Other Bi-Metallic Systems. Catalysts 2013;3:563-83.

[71] Hua B, Li M, Zhang YQ, Chen J, Sun YF, Yan N, et al. Facile Synthesis of Highly Active and Robust Ni-Mo Bimetallic Electrocatalyst for Hydrocarbon Oxidation in Solid Oxide Fuel Cells. ACS Energy Letters 2016;1:225-30.

[72] Navarro RM, Pena M, Fierro J. Hydrogen production reactions from carbon feedstocks: fossil fuels and biomass. Chem Rev 2007;107:3952-91.

[73] Zhu H, Wang W, Ran R, Su C, Shi H, Shao Z. Iron incorporated Ni-ZrO_2 catalysts for electric power generation from methane. Int J Hydrogen Energy 2012;37:9801-8.

[74] Wang W, Zhu H, Yang G, Park HJ, Jung DW, Kwak C, et al. A NiFeCu alloy anode catalyst for direct-methane solid oxide fuel cells. J Power Sources 2014;258:134-41.

[75] Lo Faro M, Reis RM, Saglietti GGA, Zignani SC, Trocino S, Frontera P, et al. Investigation of Ni-based alloy/CGO electro-catalysts as protective layer for a solid oxide fuel cell anode fed with ethanol. J Appl Electrochem 2015;45:647-56.

[76] Yoon D, Manthiram A. Ni-M (M = Sn and Sb) intermetallic-based catalytic functional layer as a built-in safeguard for hydrocarbon-fueled solid oxide fuel cells. Journal of Materials Chemistry A 2015;3:21824-31.

[77] Wang W, Su C, Wu Y, Ran R, Shao Z. Progress in solid oxide fuel cells with nickel-based anodes operating on methane and related fuels. Chem Rev 2013;113:8104-

51.

[78] Mishra A, Dudek R, Gaffney A, Ding D, Li F. Spinel oxides as coke-resistant supports for NiO-based oxygen carriers in chemical looping combustion of methane. Catal Today 2019.

[79] Wang T, Wang J, Sun Y, Duan Y, Sun S, Hu X, et al. Origin of electronic structure dependent activity of spinel $ZnNi_xCo_{2-x}O_4$ oxides for complete methane oxidation. Applied Catalysis B: Environmental 2019;256:117844-53.

[80] Kim H, Eissa AA-S, Kim SB, Lee H, Kim W, Seo DJ, et al. One-pot synthesis of a highly mesoporous $Ni/MgAl_2O_4$ spinel catalyst for efficient steam methane reforming: influence of inert annealing. Catalysis Science & Technology 2021;11:4447-58.

[81] Yang L, Bukhovko MP, Malek A, Li L, Jones CW, Agrawal PK, et al. Steam reforming kinetics of olefins and aromatics over Mn-Cr-O spinel oxides. J Catal 2021.

[82] Jin C, Yang C, Zhao F, Coffin A, Chen F. Direct-methane solid oxide fuel cells with $Cu_{1.3}Mn_{1.7}O_4$ spinel internal reforming layer. Electrochem Commun 2010;12:1450-2.

[83] Hua B, Li M, Chi B, Jian L. Enhanced electrochemical performance and carbon deposition resistance of Ni-YSZ anode of solid oxide fuel cells by in situ formed Ni-MnO layer for CH4on-cell reforming. J Mater Chem A 2014;2:1150-8.

[84] Hua B, Li M, Zhang W, Pu J, Chi B, Jian L. Methane On-Cell Reforming by Alloys Reduced from $Ni_{0.5}Cu_{0.5}Fe_2O_4$ for Direct-Hydrocarbon Solid Oxide Fuel Cells. J

Electrochem Soc 2014;161:569-75.

[85] Hua B, Li M, Pu J, Chi B, Jian L. $BaZr_{0.1}Ce_{0.7}Y_{0.1}Yb_{0.1}O_{3-\delta}$ enhanced coking-free on-cell reforming for direct-methane solid oxide fuel cells. Journal of Materials Chemistry A 2014;2:12576-82.

[86] Hua B, Li M, Luo Jl, Pu J, Chi B, Li J. Carbon-resistant Ni-$Zr_{0.92}Y_{0.08}O_{2-\delta}$ supported solid oxide fuel cells using Ni-Cu-Fe alloy cermet as on-cell reforming catalyst and mixed methane-steam as fuel. J Power Sources 2016;303:340-6.

[87] Wu XY, Tan W, Lu C, Zhang X, Li M, Fang Q, et al., Efficiency of Nickel/Yttria Stabilized Zirconia Anode-supported Solid Oxide Fuel Cell with $MnFe_2O_4$ Barrier Layer, Mater Rep 2019;33:1949-54.

[88] Zhao J, Xu X, Zhou W, Zhu Z. An in situ formed MnO-Co composite catalyst layer over Ni-$Ce_{0.8}Sm_{0.2}O_{2-x}$ anodes for direct methane solid oxide fuel cells. Journal of Materials Chemistry A 2017;5:6494-503.

[89] Zhang Y, Chen B, Guan D, Xu M, Ran R, Ni M, et al. Thermal-expansion offset for high-performance fuel cell cathodes. Nature 2021;591:246-51.

[90] Rahman IZ, Raza MA, Rahman MA. Perovskite Based Anode Materials for Solid Oxide Fuel Cell Application: A Review. Advanced Materials Research 2012;445:497-502.

[91] Huang B, Zhu Xj, Hu Wq, Wang Yy, Yu Qc. Characterization of the Ni-ScSZ anode with a LSCM-CeO_2 catalyst layer in thin film solid oxide fuel cell running on ethanol fuel. J Power Sources 2010;195:3053-9.

[92] Wang Z, Wang Z, Yang W, Peng R, Lu Y. Carbon-tolerant solid oxide fuel cells

using $NiTiO_3$ as an anode internal reforming layer. J Power Sources 2014;255:404-9.

[93] Mirzababaei J, Chuang S. $La_{0.6}Sr_{0.4}Co_{0.2}Fe_{0.8}O_3$ Perovskite: A Stable Anode Catalyst for Direct Methane Solid Oxide Fuel Cells. Catalysts 2014;4:146-61.

[94] Lv X, Chen H, Zhou W, Cheng F, Li SD, Shao Z. Direct-methane solid oxide fuel cells with an in situ formed Ni-Fe alloy composite catalyst layer over Ni-YSZ anodes. Renewable Energy 2020;150:334-41.

[95] Yang Y, Yang Z, Chen Y, Chen F, Peng S. A Promising Composite Anode for Solid Oxide Fuel Cells: $Sr_2FeMo_{0.65}Ni_{0.35}O_{6-\delta}$-$Gd_{0.1}Ce_{0.9}O_{2-\delta}$. J Electrochem Soc 2019;166:109-13.

[96] Kim HJ, Kil MJ, Lee J, Yang BC, Go D, Lim Y, et al. Ru/Samaria-doped ceria gradient cermet anode for direct-methane solid oxide fuel cell. Appl Surf Sci 2021;538:148105-12.

[97] Fan W, Sun Z, Bai Y, Wu K, Cheng Y. Highly Stable and Efficient Perovskite Ferrite Electrode for Symmetrical Solid Oxide Fuel Cells. ACS Appl Mater Interfaces 2019;11:23168-79.

[98] Yang C, Li J, Lin Y, Liu J, Chen F, Liu M. In situ fabrication of CoFe alloy nanoparticles structured $(Pr_{0.4}Sr_{0.6})_3(Fe_{0.85}Nb_{0.15})_2O_7$ ceramic anode for direct hydrocarbon solid oxide fuel cells. Nano Energy 2015;11:704-10.

[99] Yang Y, Wang Y, Yang Z, Lei Z, Jin C, Liu Y, et al. Co-substituted $Sr_2Fe_{1.5}Mo_{0.5}O_{6-\delta}$ as anode materials for solid oxide fuel cells: Achieving high performance via nanoparticle exsolution. J Power Sources 2019;438:226989-96.

[100] Yang Z, Chen Y, Xu N, Niu Y, Han M, Chen F. Stability Investigation for Symmetric Solid Oxide Fuel Cell with $La_{0.4}Sr_{0.6}Co_{0.2}Fe_{0.7}Nb_{0.1}O_{3-\delta}$ Electrode. J Electrochem Soc 2015;162:718-21.

[101] Suzuki T, Yamaguchi T, Hamamoto K, Fujishiro Y, Awano M, Sammes N. A functional layer for direct use of hydrocarbonfuel in low temperature solid-oxidefuelcells. Energy Environ Sci 2011;4:940-3.

[102] Zhao J, Xu X, Li M, Zhou W, Liu S, Zhu Z. Coking-resistant $Ce_{0.8}Ni_{0.2}O_{2-\delta}$ internal reforming layer for direct methane solid oxide fuel cells. Electrochim Acta 2018;282:402-8.

[103] Yuan X, Chen H, Tian W, Shi J, Zhou W, Cheng F, et al. Utilization of low-concentration coal-bed gas to generate power using a core-shell catalyst-modified solid oxide fuel cell. Renewable Energy 2020;147:602-9.

[104] Saunders JEA, Davy MH. In-situ studies of gas phase composition and anode surface temperature through a model DIR-SOFC steam-methane reformer at 973.15 K. Int J Hydrogen Energy 2013;38:13762-73.

[105] Pillai M, Lin Y, Zhu H, Kee RJ, Barnett SA. Stability and coking of direct-methane solid oxide fuel cells: Effect of CO_2 and air additions. J Power Sources 2010;195:271-9.

[106] Chang H, Chen H, Shao Z, Shi J, Bai J, Li S-D. In situ fabrication of (Sr,La)FeO_4 with CoFe alloy nanoparticles as an independent catalyst layer for direct methane-based solid oxide fuel cells with a nickel cermet anode. Journal of Materials Chemistry A 2016;4:13997-4007.

[107] Chang H, Chen H, Yang G, Zhou W, Bai J, Li S, et al. Enhanced coking resistance of a Ni cermet anode by a chromates protective layer. Journal of Energy Chemistry 2019;37:117-25.

[108] Chang H, Chen H, Yang G, Shi J, Zhou W, Bai J, et al. Enhanced coking resistance of Ni cermet anodes for solid oxide fuel cells based on methane on-cell reforming by a redox-stable double-perovskite $Sr_2MoFeO_{6-\delta}$. International Journal of Energy Research 2018;43:2527-37.

[109] Zhao K, Hou X, Bkour Q, Norton MG, Ha S. NiMo-ceria-zirconia catalytic reforming layer for solid oxide fuel cells running on a gasoline surrogate. Applied Catalysis B: Environmental 2018;224:500-7.

[110] Chen H, Wu Y, Yang G, Shi J, Zhou W, Bai J, et al. Direct Power Generation from Low Concentration Coal-Bed Gas by a Catalyst-Modified Solid Oxide Fuel Cell. ChemElectroChem 2018;5:1459-66.

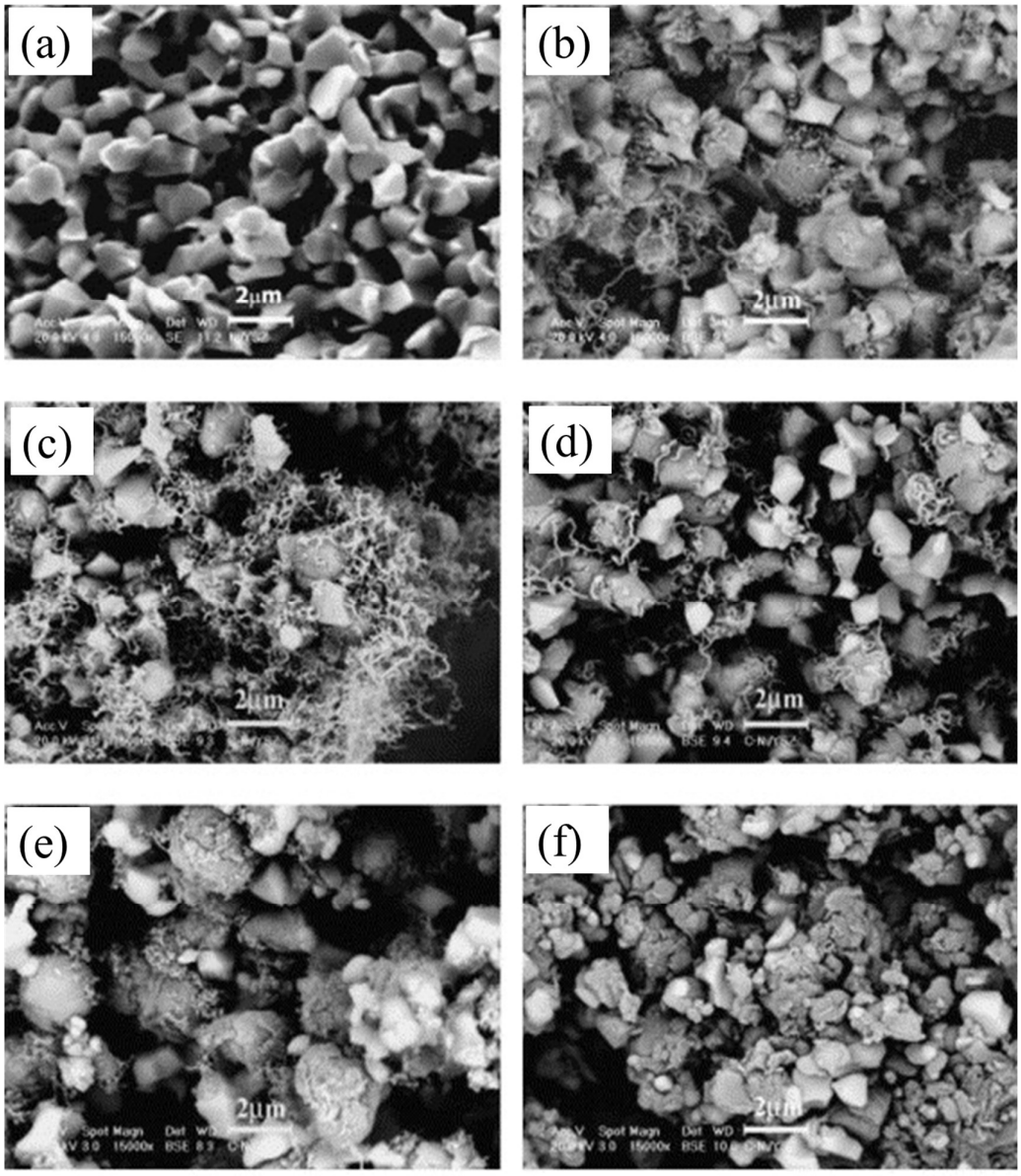

Fig. 1. SEM images of Ni/YSZ (a) as-prepared, and after carbon deposition in humidified methane for 4 h at (b) 773 K, (c) 873 K, surface, (d) 873 K, (e) 973 K, and (f) 1073 K. All images are from the centre of the pellet except for (c), reprinted with permission from Ref. [14].

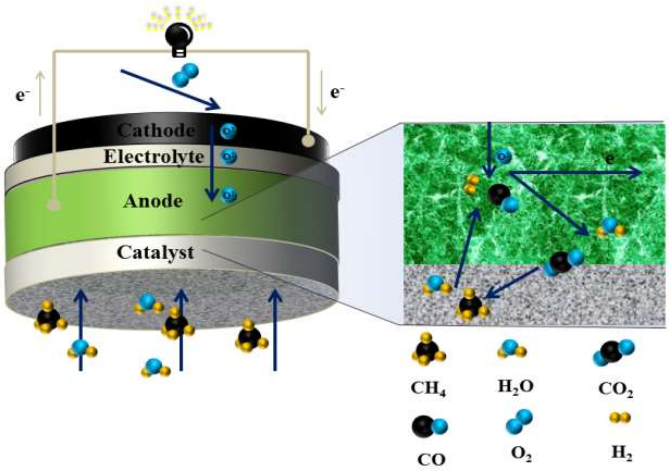

Fig. 2. Schematic showing the direct-loaded catalyst layer

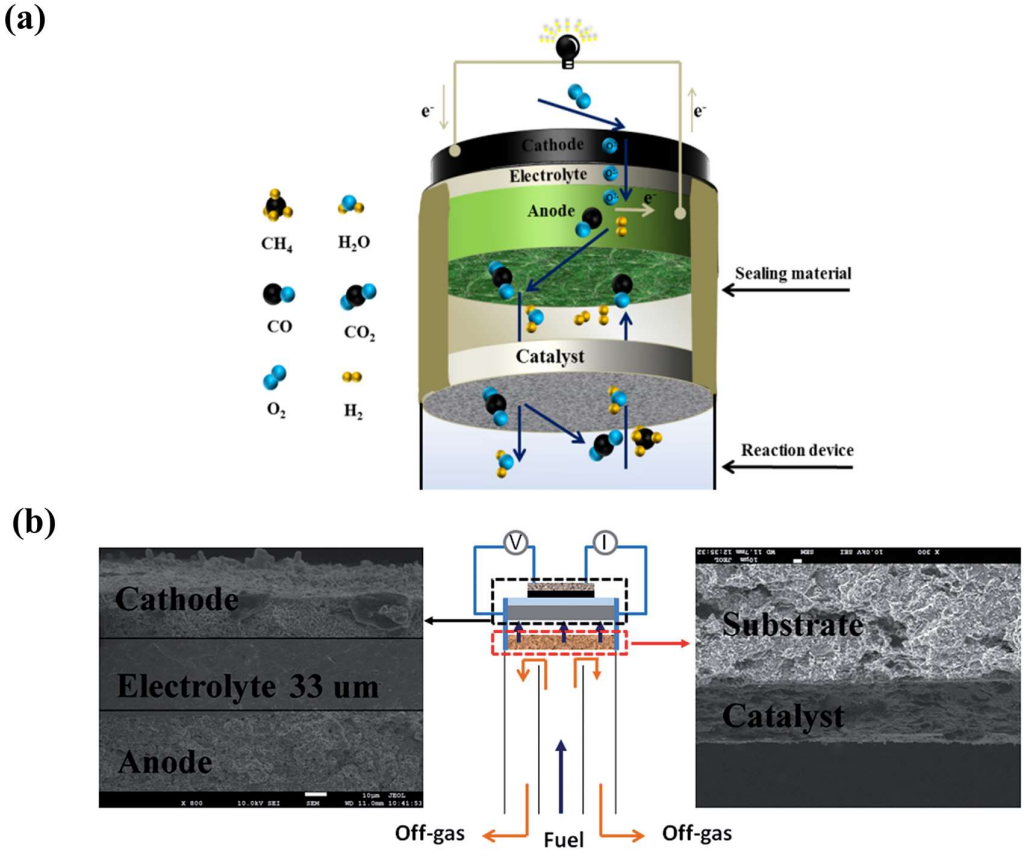

Fig. 3. (a) Schematic showing the independent catalyst layer and (b) the illustration of the cell with an independent catalyst layer, reprinted with permission from Ref. [106].

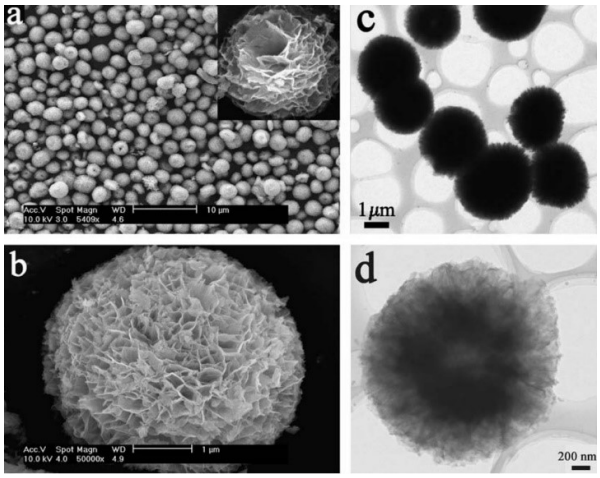

Fig. 4. Representative SEM images (a, b) and TEM images (c, d) of the flowerlike mesoporous CeO_2 microspheres. The inset in (a) is a fractured CeO_2 microsphere, reprinted with permission from Ref. [37].

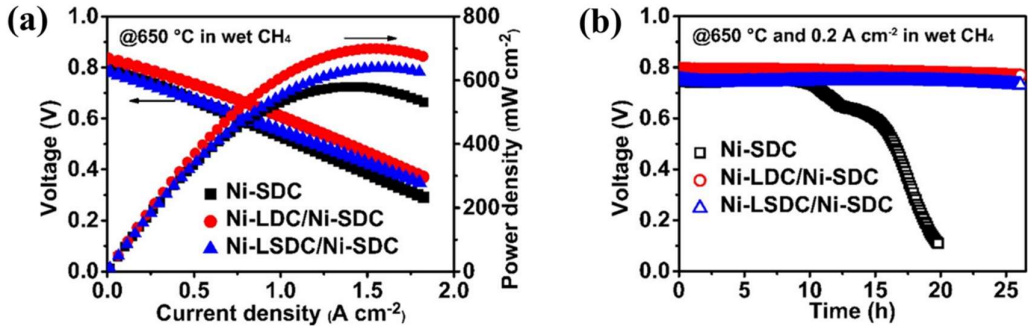

Fig. 5. (a) I-V(P) curves and (b) stability of the conventional SOFC and the SOFCs with Ni-LDC and Ni-LSDC catalyst layers at 650 °C in wet CH_4, reprinted with permission from Ref. [54].

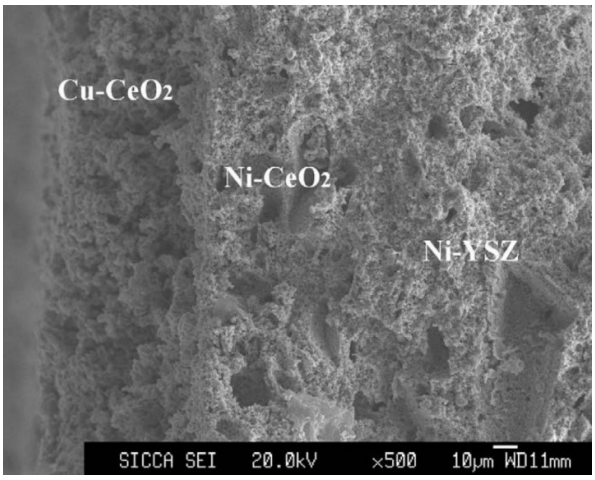

Fig. 6. The cross-sectional SEM image of cell showing interfaces of three layers in the anode after operation in ethanol for 250 h, reprinted with permission from Ref. [61].

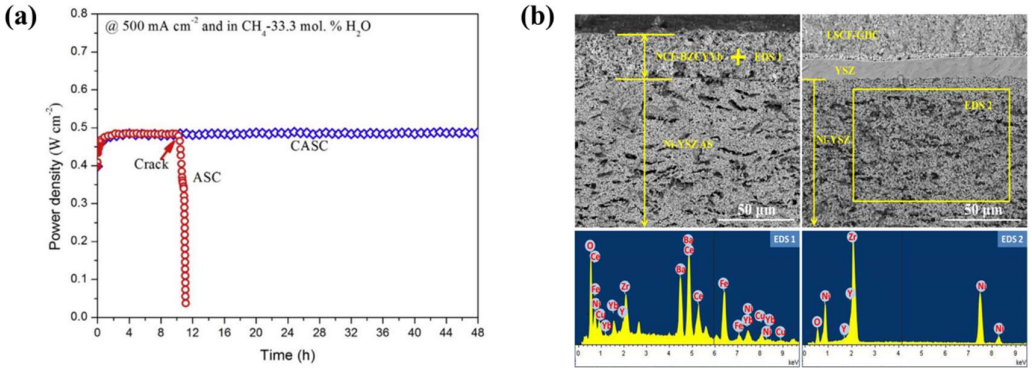

Fig. 7. (a) Time dependence of power density for the ASC and CASC fueled by CH_4-33.3 mol% H_2O atmosphere at 800 °C and 500 mA/cm^2 ; (b) Cross-sectional microstructure and compositional analysis of the CASC tested in CH_4-33.3 mol. % H_2O atmosphere at 800 °C and 500mA cm^{-2} for 48 h, reprinted with permission from Ref. [86]. Note: The cells with and without the layer of NCF-BZCYYb catalyst were designated as CASC and ASC, respectively.

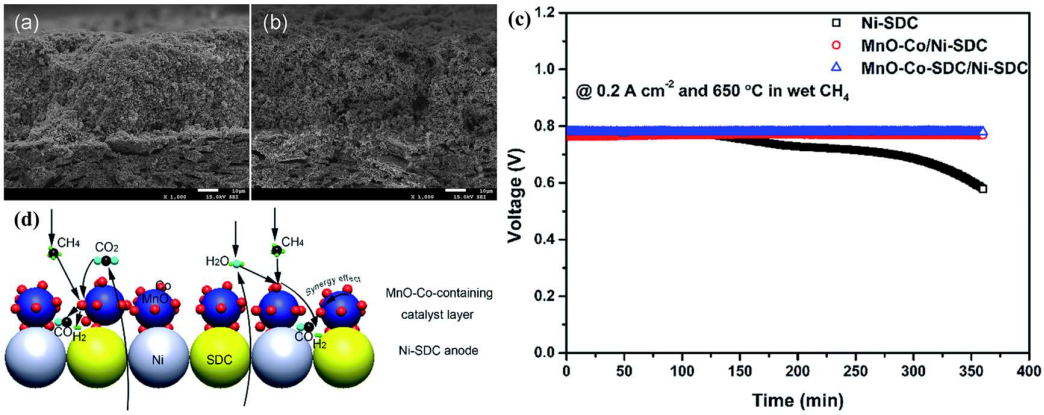

Fig. 8. (a) Cross-sectional images of MnO-Co catalyst layer/Ni-SDC anode and (b) MnO-Co-SDC catalyst layer/Ni-SDC anode interfaces after test. (c) Stability of Ni-SDC anode-supported SOFCs with and without MnO-Co and MnO-Co-SDC catalyst layers in wet methane at 0.2 A cm^{-2} and 650 °C. (d) Schematic diagram of the SOFCs with the MnO-Co-containing catalyst layer, reprinted with permission from Ref. [88].

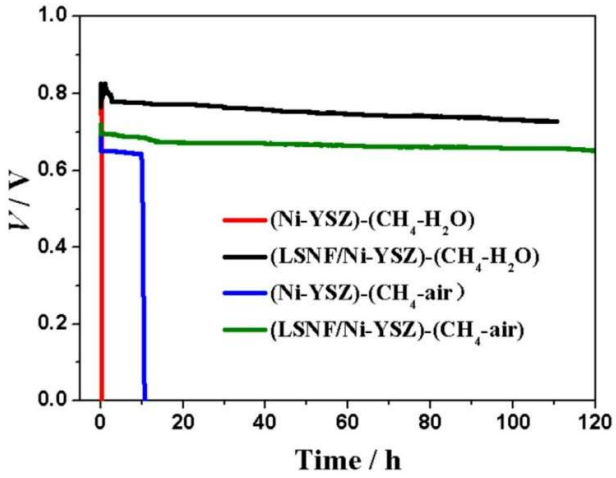

Fig. 9. Durability of Ni-YSZ and LSFN/Ni-YSZ using CH_4-H_2O fuel and CH_4-air fuel at a current of 335 mA/cm^2 at 800 °C, reprinted with permission from Ref. [94].

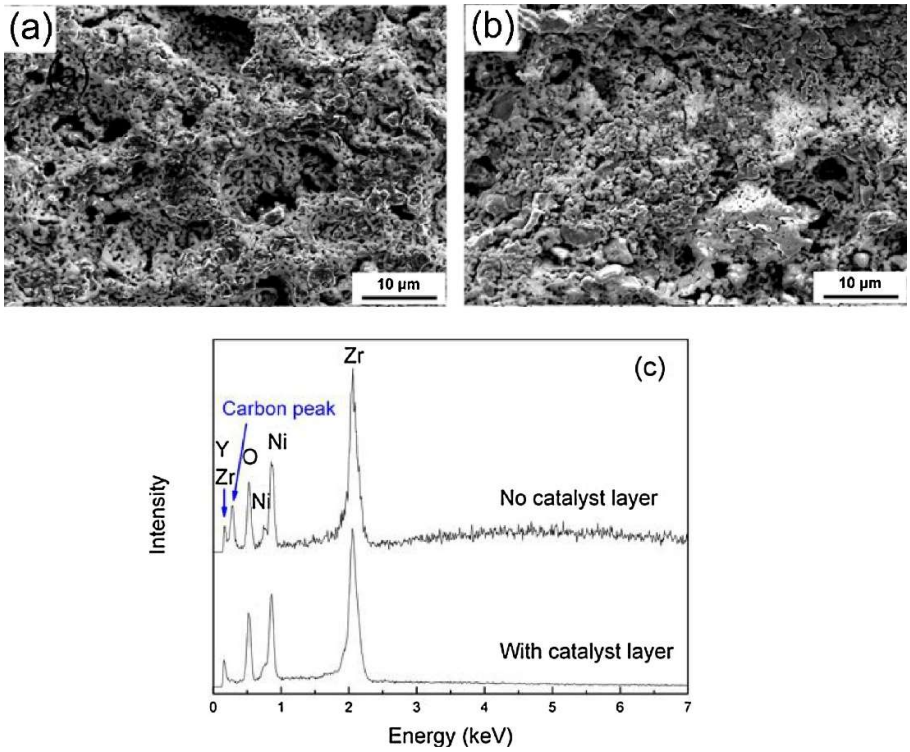

Fig. 10. SEM images of the Ni-YSZ cermet (the surface of the anode) after the performance stability measurement: (a) with the catalyst layer and (b) without the catalyst layer. (c) EDX analyses from (a) and (b), reprinted with permission from Ref. [109].

Table 1. The performance of SOFCs with/without a direct-loaded catalyst layer

Material type	Catalyst layer	Anode	Fuel	Temperature (°C)	PPD (mW/cm^2)	Time-dependent voltage (current density/ power density) of the cell with the catalyst layer (h)	Time-dependent voltage (current density/power density) of the cell without the catalyst layer (h)	Refs.
Noble metal-based materials	Ru/CeO_2	Ni-YSZ	5% C_8H_{18}+9% air +86% CO_2	770	600	50	-	[26]
	Ru/Al_2O_3	Ni-YSZ	CH_4+O_2(4:1)	750	581	～7	-	[36]
	Ru/CeO_2	Ni-SDC	5% C_8H_{18}+9% air+3% H_2O+83% CO_2	600	654	-	-	[37]
	Ru/SDC	Ni-SDC	CH_4(3% H_2O)	650	462	-	-	[38]
	Ir/CGO	Ni-YSZ	C_2H_5OH	850	-	650 (Time-dependent current density)	-	[39]
	Pd	Ni-YSZ	C_2H_5OH	750	196	59	6	[40]
	Ni/Al_2O_3	Ni-ScSZ	CH_4	850	382	2.5 (Time-dependent power density)	1.5 (Time-dependent power density)	[48]
Nickel-based materials	$LiLaNi/Al_2O_3$	Ni-ScSZ	80% CH_4+20% O_2	850	538	-	-	[51]
	$Ni/Li_{0.33}La_{0.56}TiO_3$	Ni-$(Y_2O_3)_{0.1}$ $(ZrO_2)_{0.9}$	CH_4(3% H_2O)	650	688	160	55	[52]
	$LiLaNiCu/Al_2O_3$	Ni-YSZ	80% CH_4+20% O_2	850	1081	～7	-	[53]
	$Ni/La_2Ce_2O_7$	Ni-SDC	CH_4(3% H_2O)	650	699	26	20	[54]

Table 1. The performance of SOFCs with/without a direct-loaded catalyst layer

Material type	Catalyst layer	Anode	Fuel	Temperature (°C)	PPD (mW/cm^2)	Time-dependent voltage (current density/ power density) of the cell with the catalyst layer (h)	Time-dependent voltage (current density/ power density) of the cell without the catalyst layer (h)	Refs.
Copper-based materials	Cu/CeO_2	Ni-YSZ	$C_2H_5OH+H_2O$	800	566	80 (Time-dependent power density)	-	[60]
	$Cu/CeO_2+Ni/CeO_2$	Ni-YSZ	$C_2H_5OH+H_2O$	750	-	250 (Time-dependent power density)	-	[61]
	$Cu/(ZnO-Al_2O_3)$	Ni-GDC	$C_2H_5OH+O_2$ (0.45:1)	450	50	-	-	[63]
Nickel-based alloy materials	$Ni4Fe1/ZrO_2$	Ni-YSZ	80% CH_4+20% O_2	850	1038	-	-	[73]
	$NiFeCu/ZrO_2$	Ni-YSZ	80% CH_4+20% O_2	650	334	100	-	[74]
	NiCo/CGO	Ni-YSZ	C_2H_5OH	800	550	-	-	[75]
	SbNi/GDC	Ni-GDC	CH_4	650	550	>200	～100	[76]
Spinel-based materials	$Cu_{1.3}Mn_{1.7}O_4$-SDC	Ni-GDC	CH_4(3% H_2O)	650	242	60	16	[82]
	$MnNi_2O_4$	Ni-YSZ	CH_4(20% H_2O)	800	-	24	12	[83]
	NCFO-CGO	Ni-YSZ	CH_4(7% H_2O)	800	-	24	～8	[84]
	NCFO-BZCYYb	Ni-YSZ	CH_4(33.3% H_2O)	800	1638	48 (Time-dependent power density)	11 (Time-dependent power density)	[86]

Table 1. The performance of SOFCs with/without a direct-loaded catalyst layer

Material type	Catalyst layer	Anode	Fuel	Temperature (°C)	PPD (mW/cm^2)	Time-dependent voltage of the cell with the catalyst layer (h)	Time-dependent voltage of the cell without the catalyst layer (h)	Refs.
Spinel-based materials	$MnFe_2O_4$	Ni-YSZ	Simulated bio-syngas	750	432	24	24	[87]
	$Mn_{1.5}Co_{1.5}O_4$-SDC	Ni-GDC	CH_4(3% H_2O)	650	701	15	6	[88]
Perovskite-based materials	LSCM-CeO_2	Ni-ScSZ	C_2H_5OH-H_2O(2:1)	700	238	216	-	[91]
	$NiTiO_3$	Ni-YSZ	C_3H_8(3% H_2O)	700	153	26	1	[92]
	LSCF	Ni-YSZ	CH_4	750	-	475	3 8	[93]
	LSFN	Ni-YSZ	CH_4(3% H_2O)	800	421	110	0.3	[94]
Other types of materials	CeO_2	Ni-GDC	CH_4+H_2O	554	450	-	-	[101]
	$Ce_{0.8}Ni_{0.2}O_{2-\delta}$	Ni-SDC	CH_4(3% H_2O)	650	664	40	26	[102]
	NiO-BaO-CeO_2@SiO_2	Ni-YSZ	30% CH_4+70% air	800	938	160	8	[103]

Note: YSZ: $(Y_2O_3)_{0.08}(ZrO_2)_{0.92}$; SDC: $Ce_{0.8}Sm_{0.2}O_{1.9}$; ScSZ: $(Sc_2O_3)_{0.1}(ZrO_2)_{0.9}$; GDC: $Gd_{0.2}Ce0.8O_{1.9}$; CGO: $Ce_{0.9}Gd_{0.1}O_{2-x}$; NCFO: $Ni_{0.5}Cu_{0.5}Fe_2O_4$; BZCYYb: $BaZr_{0.1}Ce_{0.7}Y_{0.1}Yb_{0.1}O_{3-\delta}$; LSCM: $La_{0.75}Sr_{0.25}Cr_{0.5}Mn_{0.5}O_3$; LSFN: $La_{0.7}Sr_{0.3}Fe_{0.8}Ni_{0.2}O_{3-\delta}$; Simulated bio-syngas: 35.5% H_2+23.79% CO+3.95% CH_4+1.19% C_2H_4+1.55% C_2H_6+3.59% CO_2+30.43% N_2

Table 2. The performance of SOFCs with/without an independent catalyst layer

Catalyst layer	Anode	Fuel	Temperature (°C)	PPD (mW/cm^2)	Time-dependent voltage of the cell with the catalyst layer (h)	Time-dependent voltage of the cell without the catalyst layer (h)	Refs.
LSCF	Ni-YSZ	CH_4(3% H_2O)	800	360	116	0.33	[106]
$La_{0.7}Sr_{0.3}Cr_{0.8}Fe_{0.2}O_{3-\delta}$	Ni-YSZ	CH_4(3% H_2O)	850	660	100	0.5	[107]
$Sr_2MoFeO_{6-\delta}$	Ni-YSZ	CH_4(3% H_2O)	800	420	55	0.33	[108]
NiMo/CeO_2·ZrO_2	Ni-YSZ	C_8H_{18}+air(1:20)	750	405	12	12	[109]
NiO-BaO-CeO_2	Ni-YSZ	30% CH_4+70% air	800	440	55	4	[110]